Metal ions turn on a stereoselective nonenzymatic reduction of keto acids by the coenzyme NADH

Robert Josef Mayer, Joseph Moran

Chem

CellPress
OPEN ACCESS

Article

Metal ions turn on a stereoselective nonenzymatic reduction of keto acids by the coenzyme NADH

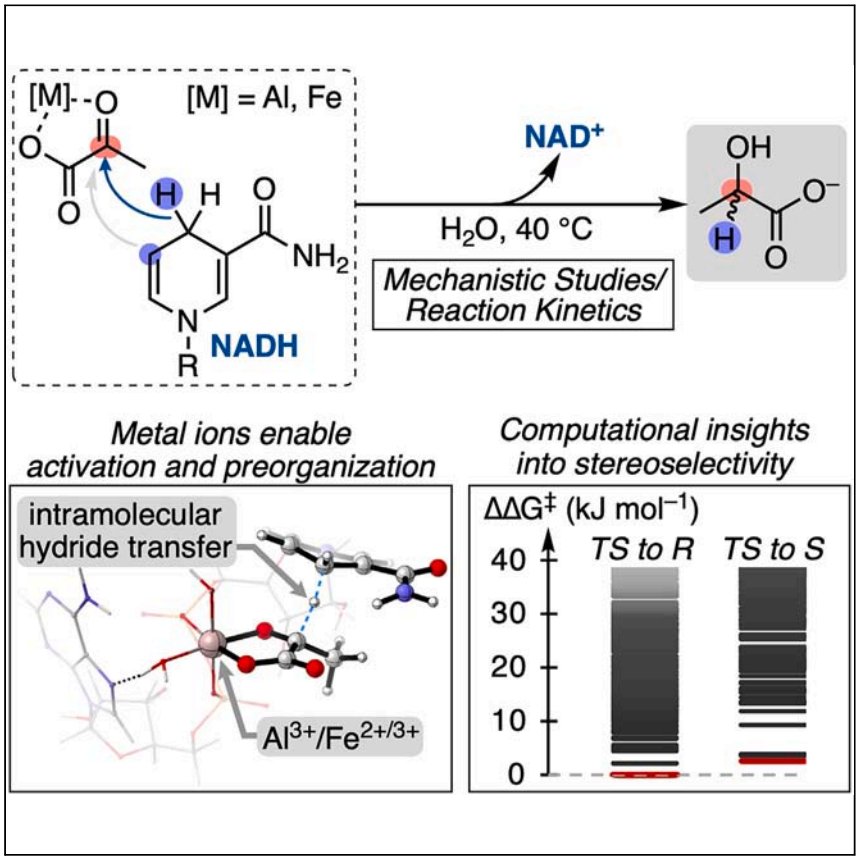

We show that metal ions catalyze the reduction of keto acids by the coenzyme NADH in water, a reaction that otherwise requires complex enzymes to proceed. The reaction is partially stereoselective, as NADH is a chiral hydride donor, yielding hydroxy acids with small to moderate enantiomeric excess. Analysis of the reaction mechanism by experiments and computations illustrates that the metal ions mimic multiple roles of enzymes by activating the substrates and pre-organizing them for an intramolecular reaction.

Robert J. Mayer, Joseph Moran

robert.j.mayer@tum.de (R.J.M.)
moran@unistra.fr (J.M.)

Highlights

The synergy of metal ions and the coenzyme NADH links genetic molecules to early metabolism

Demonstration of chirality transfer in a nonenzymatic metabolic reaction

Metal ions enable the activation and preorganization of substrates instead of enzymes

Computational insights into the mechanism and selectivity of chirality transfer

Mayer & Moran, Chem *10*, 1–13
August 8, 2024
https://doi.org/10.1016/j.chempr.2024.05.007

Please cite this article in press as: Mayer and Moran, Metal ions turn on a stereoselective nonenzymatic reduction of keto acids by the coenzyme NADH, Chem (2024), https://doi.org/10.1016/j.chempr.2024.05.007

Chem

CellPress
OPEN ACCESS

Article

Metal ions turn on a stereoselective nonenzymatic reduction of keto acids by the coenzyme NADH

Robert J. Mayer[1,2,*] and Joseph Moran[1,3,4,5,*]

SUMMARY

The relationship between genetic molecules and metabolism is one of the longest-standing problems for the origin of life. A central molecule within early metabolism is the coenzyme nicotinamide adenine dinucleotide (NAD(H)), a modified ribonucleotide and reducing agent. Yet, without enzymes, NADH does not reduce carbonyl compounds, its primary metabolic substrates, leading to an apparent paradox regarding its role in the evolution of metabolism. We now report that abundant metal ions turn on a nonenzymatic, stereoselective, and potentially primordial reduction reaction of keto acids by NADH. Kinetic, mechanistic, and computational studies elucidate the reaction mechanism and the way stereochemistry is transferred. Complexes of metals with RNA-derived coenzymes could have mediated the transition from inorganic to organic reducing agents and the propagation of chirality in early metabolism.

INTRODUCTION

Coenzymes are thought to have played a crucial role in the emergence of metabolism and, ultimately, life, even before the existence of enzymes.[1–5] Of the many known coenzymes, nicotinamide adenine dinucleotide (NAD) is essential for today's biochemical metabolism, where it is involved in most oxidation and reduction reactions.[6–8] NAD contains both a ribosylated nicotinamide and an adenosine diphosphate moiety within its structure and, therefore, constitutes a bridge between metabolism and genetic polymers. According to bioinformatic analyses, NAD is thought to be the central coenzyme within the metabolism of the last universal common ancestor (LUCA) and is assumed to be one of the most ancient coenzymes.[9–11] Identifying nonenzymatic reactions involving the NAD coenzyme is thus of central importance to explaining the onset of metabolism from prebiotic chemistry. According to models for the emergence of metabolism, the key role of NAD is to mediate the transition from inorganic to organic reducing agents (Figure 1). Hydrogen, an inorganic reductant, is thought to have been the primary energy source of the LUCA and is still used by some bacteria or archaea. However, hydrogen fails to reduce the majority of organic molecules without transition metal catalysts.[12] In both prebiotic chemistry and biocatalysis, extensive research has identified conditions that allow the reduction of NAD^+ to NADH.[13–18] Once formed, NADH is then thought to have acted as an organic reducing agent within the early stages of metabolism.

Attempts to synthesize the nicotinamide skeleton and derivatives under potentially prebiotic conditions date back to the early 70s,[19–22] and various isomers of nicotinic acid and nicotinamide have even been detected in meteorites.[23] Plausible prebiotic syntheses for ribonucleotides (RNA), including that of the adenosine fragment of

THE BIGGER PICTURE

Coenzymes are thought to have played a central role in the emergence of metabolism. However, studies in the context of prebiotic chemistry face the problem that outside of enzymes, many such coenzymes do not react with their biological substrates. Previous work suggests nicotinamide adenine dinucleotide (NAD) to be one of the most ancient coenzymes and to be central to early metabolism. Yet, these models suffer from the logical gap that without enzymes, the reduced coenzyme NADH does not react with keto acids, some of its primary biological substrates.

We now report that aluminum or iron ions are catalysts for the reduction of keto acids by NADH. The ions mimic some of the roles of enzymes, such as the activation of substrates and the preorganization of keto acids with NADH. Moreover, the reaction proceeds with moderate stereoselectivity. Our work gives insight into how an important coenzyme could have participated in a primitive metabolism that predated enzymes.

Please cite this article in press as: Mayer and Moran, Metal ions turn on a stereoselective nonenzymatic reduction of keto acids by the coenzyme NADH, Chem (2024), https://doi.org/10.1016/j.chempr.2024.05.007

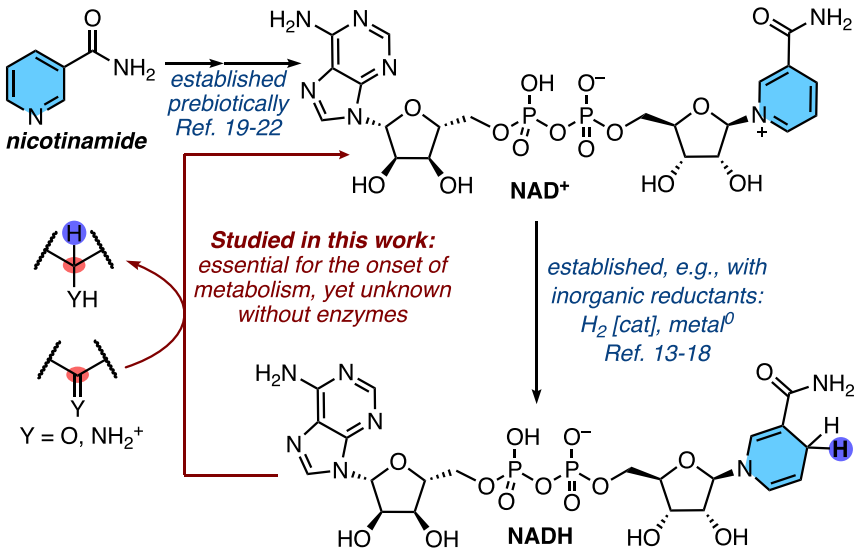

Figure 1. Role of NADH within metabolism

NAD^+ is accessible from the *N*-glycosylation of nicotinamide and can subsequently undergo reduction to NADH. Within metabolism, NADH then acts as an organic reducing agent.

NAD^+, have also been reported,[24–26] and RNA can even catalyze the synthesis of the NAD cofactor itself.[27] NADH can donate electrons to ubiquinone within protocell models to generate proton gradients,[28] suggesting a connection between nucleotide-derived coenzymes and metabolism, and RNA was further reported to be able to catalyze electron transfer processes in conjunction with iron (II).[29] However, NADH itself does not typically act as a nucleophilic hydride donor for carbonyl compounds outside of enzymes in water, arguably its major role within metabolism. The only reported nonenzymatic hydride transfer from NADH to a carbonyl itself in water is with benzaldehyde as substrate, as indirectly deduced from kinetic data.[30] More is known about the reactivity of NADH analogs, which were found to reduce highly electrophilic trifluoroacetophenone and hexachloroacetone in aqueous acetonitrile or isopropanol.[31] Nonetheless, the lack of hydride transfer from NADH to metabolic substrates in the absence of enzymes presents a fundamental paradox in explaining the emergence of metabolism since it is crucial for synthesizing key metabolites like hydroxy- and amino acids.[32]

Catalysis is essential for reducing biochemically relevant keto acids with hydride donors, as otherwise, even under harsh reaction conditions, only traces of the product can be obtained.[33,34] However, Brønsted acid catalysis of reduction reactions is incompatible with NADH outside of enzymes due to readily occurring decomposition (Figure S78).[35] As an alternative to Brønsted acid catalysis, Lewis acidic metal ions like Zn^{2+} can activate substrates in dehydrogenase enzymes or ribozymes.[36] Similarly, metal ions allow the reduction of carbonyl groups by nicotinamide analogs in organic solvents.[37–41] We herein show that metal ions turn on a stereoselective nonenzymatic hydride transfer reaction between NADH and keto acids in water, enabling some of the key functionality nowadays held by enzymes.[42,43] We focused our investigation on keto acids as substrates, as they are obtained under plausible prebiotic conditions[44] and are the biosynthetic starting materials for the synthesis of hydroxy and amino acids, both of which are assumed to have a central role within early metabolism and the formation of peptides or analogs thereof.[45]

[1]Institut de Science et d'Ingénierie Supramoléculaires (ISIS), CNRS UMR 7006, Université de Strasbourg, 8 Allée Gaspard Monge, 67000 Strasbourg, France

[2]Department of Chemistry, School of Natural Sciences, Technical University of Munich, Lichtenbergstraße 4, 85748 Garching, Germany

[3]Institut Universitaire de France (IUF), 75005 Paris, France

[4]Department of Chemistry and Biomolecular Sciences, University of Ottawa, Ottawa, ON K1N 6N5, Canada

[5]Lead contact

*Correspondence:
robert.j.mayer@tum.de (R.J.M.),
moran@unistra.fr (J.M.)

https://doi.org/10.1016/j.chempr.2024.05.007

Please cite this article in press as: Mayer and Moran, Metal ions turn on a stereoselective nonenzymatic reduction of keto acids by the coenzyme NADH, Chem (2024), https://doi.org/10.1016/j.chempr.2024.05.007

RESULTS AND DISCUSSION

Metal-ion catalysis of keto acid reduction

We started our investigation by testing whether metal ions are, in principle, capable of acting as Lewis acid catalysts for the reduction reactions of keto acids in aqueous solutions. The previously investigated reduction of pyruvate (**1a**) to lactate (**2a**) with BH_3CN^- was chosen as a model reaction to examine the effect of different concentrations of Al^{3+} ions on the reaction rate, as the reduction with NADH does not proceed uncatalyzed (see supplemental information, section metal-ion catalysis of the reaction of pyruvate with $NaBH_3CN$ for details).[34] Al^{3+} was selected as it is stable toward reduction by BH_3CN^-, and 0.1 M acetate buffer at pH 5 was chosen for convenience due to the slow reaction rate at neutral pH.[46] Under these specific conditions and using 1 mol % ethylenediaminetetraacetate with respect to pyruvate to scavenge any metal impurities, the pseudo-first-order rate constant of the general acid-catalyzed background reaction was determined. Significantly higher reduction rates were observed in the presence of catalytic amounts of Al^{3+} ions (Figure 2A). The observed linear correlation of k_{obs} and $[Al^{3+}]$ allowed us to extrapolate the pseudo-first-order rate for a specific catalyst loading and to estimate the rate acceleration due to metal-ion catalysis. According to our extrapolation, the reaction with 100 mol % Al^{3+} with respect to pyruvate is approx. 130,000 times faster than the acid-catalyzed background reaction.

In light of these results, we performed a 96-well plate-based high-throughput screen to study how catalytic amounts of different metal ions or hydrogen bond donors promote the reduction of pyruvate by NADH at various pH values and buffer compositions (supplemental information, section exploration of experimental space of pyruvate reduction. Pyruvate (**1a**) was again chosen as a model substrate as it was previously found to be the least reactive keto acid in reductions with BH_3CN^- and is one of the universal metabolite precursors.[34] After a reaction time of 14 h at 40°C and after removing metal ions by precipitation as phosphates/sulfides (supplemental information, section removal of metal ions/validation of analytical methodology), the concentration of lactate (**2a**) was determined by ^1H NMR spectroscopy combined with software-based spectral deconvolution. As previously found, no lactate could be detected in the uncatalyzed control reaction. However, multiple metal ions were found to promote the reaction, with the highest yields being observed with Al^{3+}, $Fe^{3+/2+}$, Bi^{3+}, and V^{3+} (Figure 2B). The reasons for the low yields of lactate observed with other metals varied. In the reaction conducted in an unbuffered solution with some catalysts (e.g., [thio]urea, Mg^{2+}, Ca^{2+}), leftover NADH indicated insufficient activation of **1a**. In neutral phosphate buffer, hydrolyzed NADH was predominantly observed, and most metal ions precipitated as insoluble phosphates. Finally, some metals did not activate **1a** toward reduction but promoted its auto-aldol reaction to yield parapyruvate (e.g., Mn^{2+}).

We next set out to understand the relationship between the yield and various factors (i.e., the response surface of the reaction). We focused our further investigation on Al^{3+} and Fe^{3+} as they are among the most efficient catalysts in our screen and the two most abundant metals in the Earth's crust, making them especially relevant for a prebiotic context. The initial screening showed that the yield of **2a** in the Al^{3+} and Fe^{3+}-catalyzed reaction is only slightly affected by the pH and buffer type (Figure 2B). Under unbuffered conditions starting from $AlCl_3$ $6H_2O$ or $FeCl_3$ $6H_2O$, the pH remained between pH 4.5 and 5 during the reaction, presumably due to the buffering effect of the substrate's functional groups. Accordingly, pH, buffer type, and buffer concentration were not further investigated, and unbuffered conditions

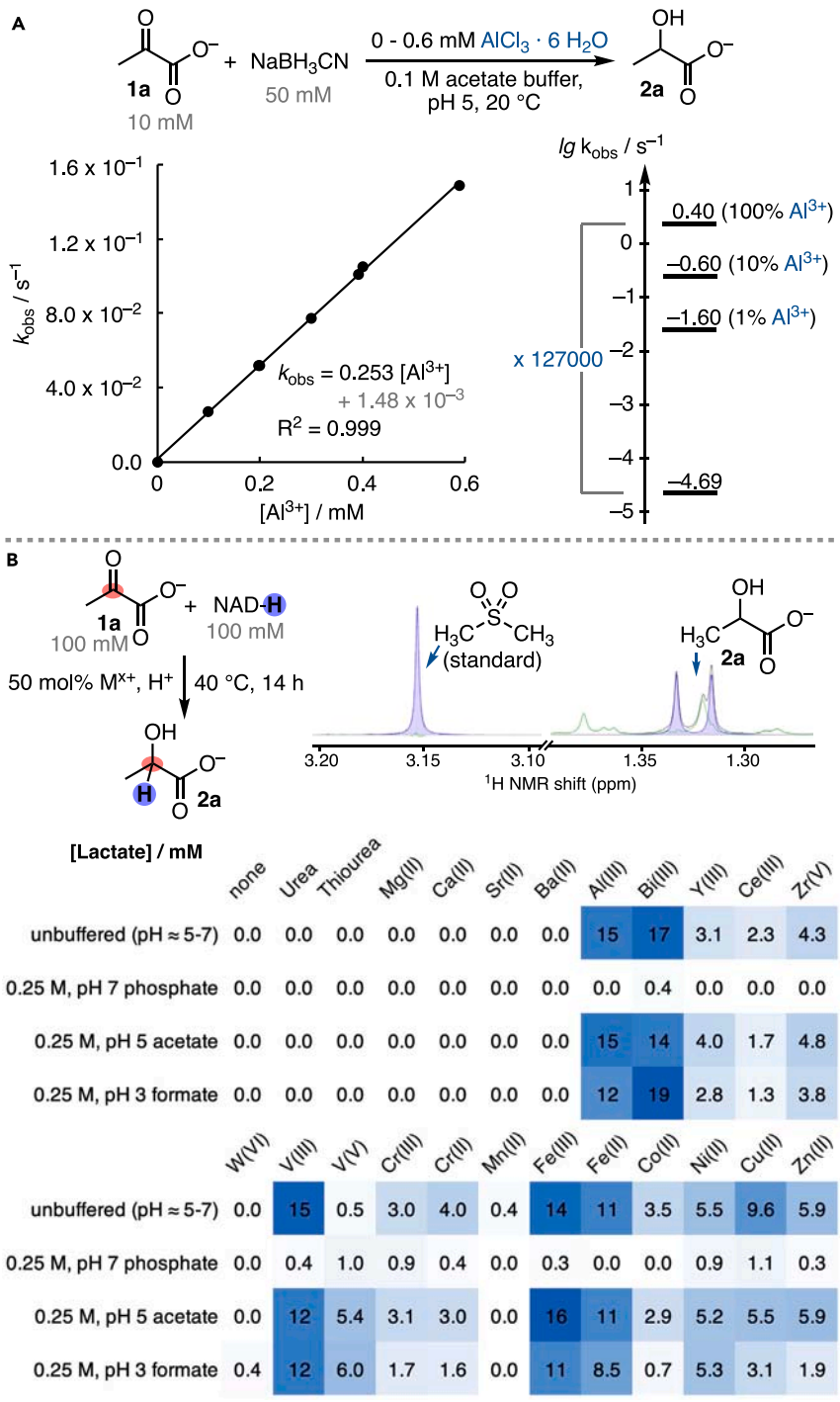

Figure 2. Metal-ion catalysis of pyruvate reduction by BH_3CN^- or NADH

(A) Kinetics of the reduction of pyruvate (**1a**) with BH_3CN^- in the presence of Al^{3+} showing the ability of Al^{3+} to act as Lewis acid catalyst.

(B) High-throughput screen of the experimental space for the reduction of pyruvate (**1a**) by NADH in the presence of various promotors.

Please cite this article in press as: Mayer and Moran, Metal ions turn on a stereoselective nonenzymatic reduction of keto acids by the coenzyme NADH, Chem (2024), https://doi.org/10.1016/j.chempr.2024.05.007

CellPress
OPEN ACCESS

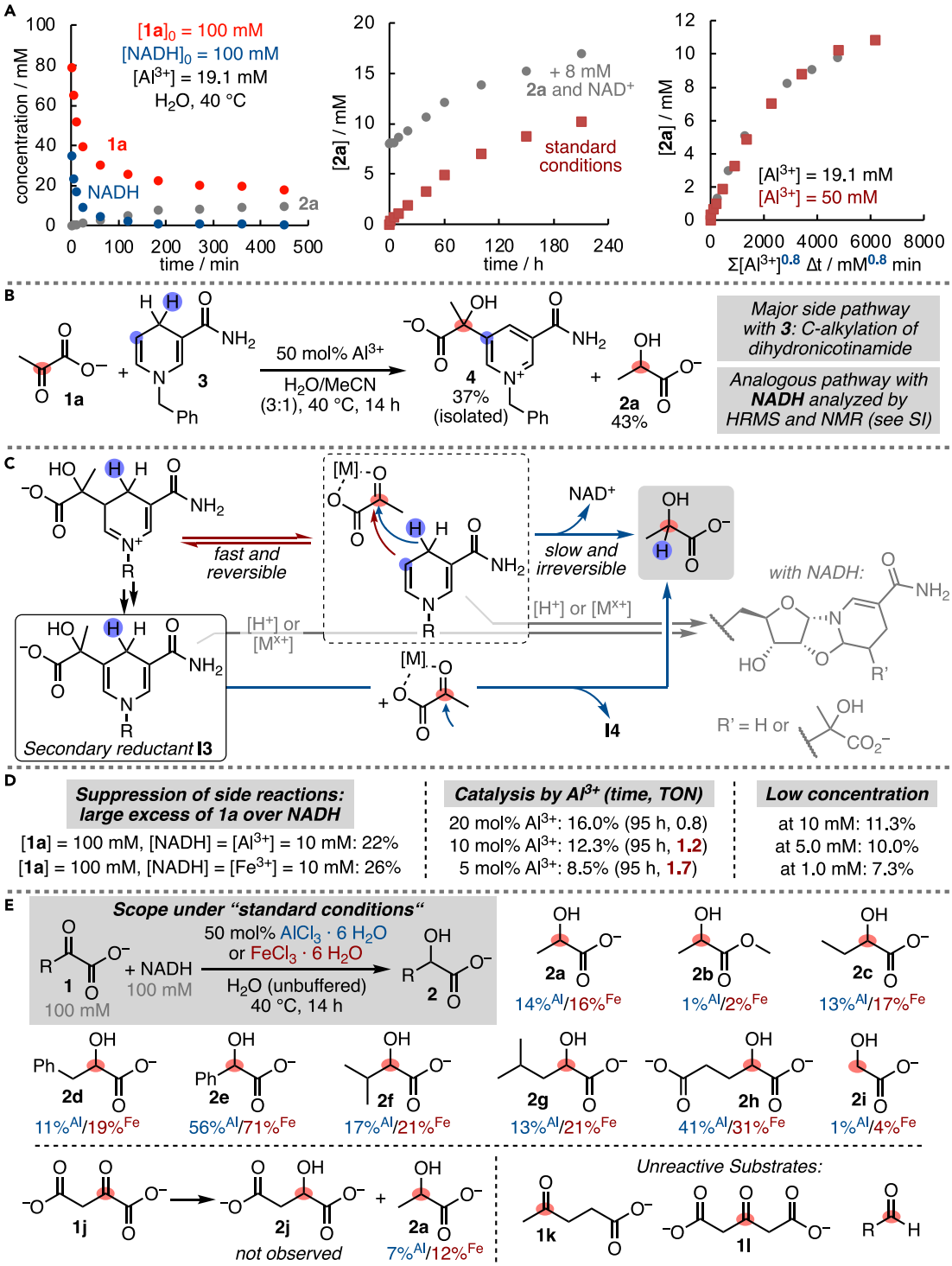

Figure 3. Kinetic and mechanistic analysis of the reaction mechanism and analysis of the reaction scope

(A) Reaction profile of the Al^{3+}-catalyzed reduction of pyruvate (**1a**) by NADH (left), reaction profile for lactate (**2a**) formation under standard conditions and in the presence of additional lactate and NAD^+ (center), and determination of the reaction order in Al^{3+} using variable time normalization analysis (VTNA, right).

(B) Product analysis of the reaction of pyruvate (**1a**) with dihydronicotinamide **3** (see supplemental information, section reaction with dihydronicotinamide 3 for details).

Please cite this article in press as: Mayer and Moran, Metal ions turn on a stereoselective nonenzymatic reduction of keto acids by the coenzyme NADH, Chem (2024), https://doi.org/10.1016/j.chempr.2024.05.007

Figure 3. *Continued*

(C) Proposed mechanistic model for the reaction of dihydronicotinamides with keto acids (see supplemental information, Figure S72 for the full pathway).

(D) Yield of lactate (**2a**; with respect to NADH in case of the excess reactions; with respect to pyruvate for the catalysis/concentration variations) under conditions deviating from the standard conditions and to evaluate catalysis efficiency with regard to lactate formation.

(E) Reaction scope under standard conditions chosen for maximizing product yield at short reaction times (see supplemental information, section reaction scope for all details. All yields are calculated with respect to the keto acid).

were chosen as the standard. A reaction time of 14 h was selected to evaluate the reaction optimization at a point where complete conversion is achieved. The remaining parameters that required optimization were the overall concentration of the reaction, the equivalents of NADH, the concentration of the catalyst, and the temperature of the reaction. To explore the response surface of the reaction with both metals, a Box-Behnken design was applied to correlate the yield with respect to pyruvate with the impact of these input parameters (supplemental information, section reaction optimization by design of experiments). The reactions with Al^{3+} and Fe^{3+} were most sensitive to temperature. Increasing temperature drastically increased the yield and selectivity of lactate formation, suggesting the involvement of reversible side processes (i.e., the competition between kinetically and thermodynamically controlled pathways). The reaction yield is inversely correlated with the NADH concentration, as with an excess of NADH, the alkylation of NADH dominates (cf. Figures 3B and 3C). The statistical model predicts one equivalent of NADH to be optimal. The control reaction of pyruvate with Al^{3+} in the absence of NADH only yielded aldol addition and condensation products, and no traces of lactate were observed (cf. supplemental information, section pyruvate decomposition under the reaction conditions [control experiment]). Notably, when taking a reaction time of 14 h as the reference point, the influence of concentration was statistically significant only for Al^{3+} and not for Fe^{3+}, and the catalyst loading was not statistically significant for either metal.

Mechanistic and kinetic studies

After the formation of lactate ceased, only traces of pyruvate could be detected, and side products account for the remaining mass balance, as analyzed with ^{13}C-labeled pyruvate by NMR and mass spectrometry (see discussion below and section side product analysis of the Al^{3+}-catalyzed reaction of NADH and pyruvate in the supplemental information). Thus, we next set out to obtain deeper insights into the reaction mechanism and the underlying constraints. First, the kinetics of the reaction were followed at 40°C in the presence of different amounts of Fe^{3+} and Al^{3+} using manual sampling (Figure 3A, left; see supplemental information section kinetic analysis of the reaction of NADH and pyruvate for details). Notably, the NADH concentration drops far faster than that of pyruvate. The lactate concentration continues to increase even after NADH is fully consumed, with the reaction eventually stalling. This observation indicates that NADH could be involved in side reactions that are either reversible (i.e., in the later stages of the reaction, lactate formation is due to a small amount of NADH that is liberated from possible adducts and immediately consumed) or that lactate is formed through the action of a different reductant that dominates in the later parts of the reaction. When lactate and NAD^+ are added from the beginning ("same excess experiment"), an identical but shifted reaction profile was observed, suggesting that the cease in conversion is not due to inhibition by **1a**/NAD^+ or catalyst deactivation (Figure 3A, center). To obtain insights into the reaction orders, we next performed a "variable time normalization analysis" (VTNA) of the kinetics of lactate formation (supplemental information, section variable time normalization analysis). Kinetic profiles for reactions with different concentrations of metal catalysts and NADH in comparison with the standard conditions were

Please cite this article in press as: Mayer and Moran, Metal ions turn on a stereoselective nonenzymatic reduction of keto acids by the coenzyme NADH, Chem (2024), https://doi.org/10.1016/j.chempr.2024.05.007

obtained by manual sampling of the reactions. Following the procedure developed by Burés, VTNA analysis allowed us to derive a positive reaction order for Al^{3+} and Fe^{3+} (Figure 3A, right, and Figure S74), in line with the expected Lewis acid activation.[47] The reaction order is, in both cases, not an integer (i.e., 1). Yet, this is not surprising given the complexity of the mechanism involving multiple side pathways (cf. discussion below) and the fact that we based our analysis on lactate formation, which only corresponds to one possible product. In agreement with the analysis of the response surface, a negative reaction order could be derived for NADH based on monitoring lactate formation (Figure S75). This suggests that the reduction of pyruvate by NADH is competing with another reversible reaction involving both compounds.

Analyzing the reaction products can provide a rationale for the observed kinetics and further to clarify the mass balance of the reaction. To simplify the search for the competing reaction, initial studies were performed on the model dihydronicotinamide **3**. Under similar reaction conditions as with NADH (cf. Figure 2), **3** yields, in addition to **2a**, the zwitterionic pyridinium species **4**, which could be isolated and characterized (Figure 3B; for the analysis of the mass balance, see supplemental information section NMR analysis of the mass balance for pyruvate reduction by 4 [rm04-645]). Further side products are acetate, stemming from the oxidative decarboxylation of pyruvate,[15] and the aldol condensation product of pyruvate, 2-methyl-4-oxopent-2-enedioic acid (OMPD). An analogous C-alkylation, as observed with **3**, was also established in the reaction of NADH with pyruvate, as detailed in the section side product analysis of the Al^{3+}-catalyzed reaction of NADH and pyruvate of the supplemental information derived from isotope labeling, mass spectrometry, and NMR studies. Based on our experimental data and previous kinetic studies of carbonyl addition to dihydronicotinamides,[31] a mechanistic model accounting for the formation of lactate and various side products can be derived (Figures 3C and S72): slow but irreversible hydride transfer competes with fast and reversible carbon attack. Kinetically favored carbon attack dominates with a large excess of NADH and at low temperatures. Thermodynamically favorable lactate formation prevails with an equimolar ratio of pyruvate and NADH at elevated temperatures. The initial carbon attack is partially reversible or yields dihydropyridine **I3** as a side product, which also acts as a reducing agent for pyruvate. Alternatively, NADH and **I3** can undergo established acid-catalyzed anomerization and ring-closure.[35] By means of oxidative decarboxylation, some of the NAD^+ formed after hydride transfer can react with pyruvate to regenerate NADH, acetate, and CO_2.[15] However, the small amounts of acetate observed do not suggest this to be a major pathway. Overall, the observed ambident reactivity, as well as acid-catalyzed decomposition of NADH, points to the important role of enzymes in achieving chemoselectivity in reactions involving NADH.

Using these mechanistic insights, the yields of lactate could be increased to 26% by using a large excess of the keto acid with respect to NADH (with the yield calculated relative to NADH), thereby reducing the extent of side pathways (Figure 3D). Moreover, with catalyst loadings as low as 5 mol % relative to pyruvate, we observed catalyst turnover for lactate formation with respect to the metal ion (up to a turnover number (TON) of 1.7), representing a rare example of catalytic turnover in a prebiotic context.[43] The reaction was also found to operate at concentrations as low as 1 mM with respect to NADH (Tables S24–S26). Rather than soluble salts, when geologically relevant iron or aluminum minerals were used as metal sources for the reduction of pyruvate, lactate was still obtained, albeit at reduced rates (up to 3.8% with FeS after 120 h, Table S27). Under these conditions, we assume that the catalytically relevant

Please cite this article in press as: Mayer and Moran, Metal ions turn on a stereoselective nonenzymatic reduction of keto acids by the coenzyme NADH, Chem (2024), https://doi.org/10.1016/j.chempr.2024.05.007

metal ions are leached out into the solution, as evident by the yellowish color of reaction solutions involving iron minerals and the subsequent precipitation of black iron sulfide upon adding sulfide/phosphate solution during the workup.

Next, we applied the reaction conditions to other common metabolites in biochemistry (Figure 3E). To obtain short and convenient reaction times and concentrations for our analysis, we maintained a 1:1 ratio of keto acid to NADH and opted for 50 mol % of metal salts with respect to the keto acid. With either Al^{3+} or Fe^{3+} as catalysts, all investigated α-keto acids (**1c**–**1h**) underwent reduction to the corresponding hydroxy acids (**2c**–**2h**) to a similar or greater extent than pyruvate (**2a**). One notable exception was glyoxylate (**1i**), which only yielded traces of glycolate (**2i**). The highest yields were observed with phenyl pyruvate (**1e**) to yield mandelic acid (**2e**). We interpret this finding with the lack of enolizable protons in **1e** and, thus, the suppression of competing aldol chemistry. Furthermore, presumably due to the steric constraints of the phenyl group, we did not observe any further side products stemming from C-5 alkylation of NADH, as readily observed with pyruvate (cf. Figure 3B). Oxaloacetate (**1j**) decarboxylates more rapidly under the reaction conditions than it undergoes reduction to malate, and exclusively **2a** was observed.

Exploring other classes of carbonyl compounds gave further insight into the mechanism. The methyl ester of pyruvate **1b** only yielded trace amounts of the reduction product **2b**, and no conversion was observed with β- or γ-keto acids **1k** and **1l**. Aldehydes (besides **2i**) and conjugated carbonyl compounds like uracil were similarly unreactive under the reaction conditions (Figure S16). The selectivity for free α-keto acids suggests that the presence of a coordinating moiety for metal ions leading to the formation of 5-membered chelates is essential for activating the carbonyl group toward NADH.

Chirality transfer and computational analysis

Asymmetric reductions of carbonyl groups by tailored dihydronicotinamides have previously been reported in organic solvents.[38,39,48] We, therefore, tested whether NADH can affect the asymmetric nonenzymatic reduction of pyruvate (**1a**) under our standard conditions with 50 mol % Al^{3+} relative to the keto acid since it is also a chiral hydride donor due to the numerous stereocenters set by the two ribose moieties and bears multiple coordination sites. To analyze the enantiomeric excess (*ee*) of **2a**, crude reaction samples were acidified, extracted with Et_2O, and the residue was derivatized with L-menthol and acetyl chloride, adapting a literature procedure.[49] The resulting diastereomeric esters were separated and quantified by gas chromatography/mass spectrometry (GC/MS) calibrated against reference compounds. With NADH, a significant preference for R-lactate formation was observed. To obtain further insights into the mechanism of the chirality transfer, we next investigated the *ee* of **2a** and the other hydroxy acids (**2c**–**2h**) as a function of the reaction time (Figure 4A). The *ee* of *R-lactate* was found to be inversely correlated with the reaction yield, and the highest *ee* was observed at the beginning of the reaction. We thus used the mono-exponential correlation of *ee* vs. time (see supplemental information, section stereochemical analysis of the reaction) to extrapolate the initial *ee* of the reaction for a consistent comparison of the intrinsic chirality transfer of NADH itself. In the case of lactate, the % *ee* at t = 0 was determined to be 33% *ee*. A set of control experiments showed that lactate does not undergo racemization under the reaction conditions and that the reaction is irreversible (supplemental information, section reaction profile of chirality transfer with pyruvate). Thus, the observed enantioselectivity is determined at the transition state. In the same way, other keto acids produced the corresponding hydroxy acids **2c**–**2h** with 16%–60% *ee* at t = 0. The

Please cite this article in press as: Mayer and Moran, Metal ions turn on a stereoselective nonenzymatic reduction of keto acids by the coenzyme NADH, Chem (2024), https://doi.org/10.1016/j.chempr.2024.05.007

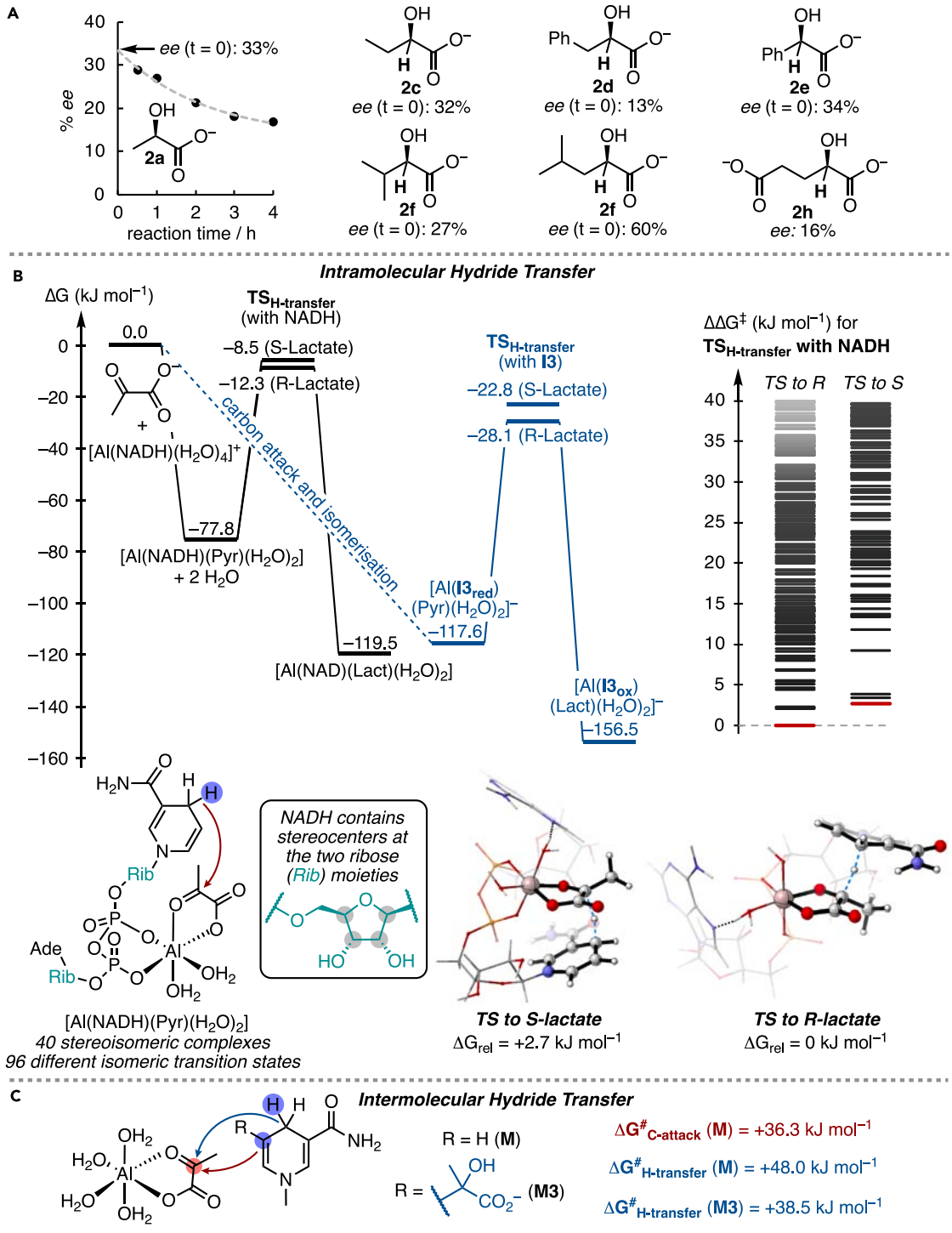

Figure 4. Observed enantioenriched hydroxy acids and computational analysis of chirality transfer

(A) Reaction profile for R-lactate formation in the reaction of pyruvate with NADH with 50 mol % Al^{3+} indicating deterioration of enantioselectivity during the reaction and initial enantiomeric excess at the beginning of the reaction derived from *ee*-time profiles.

(B) Gibbs free energy profiles for intramolecular hydride transfer within Al^{3+}-pyruvate-NADH complexes calculated at the DLPNO-CCSD(T)/cc-pVTZ//SMD(H_2O)/M06-2X/def2-SVP level of theory (left), energetic ranking of the 841 computed transition state structures leading to either R- or S-lactate within a window of 40 kJ mol^{-1} (right), and 3D-structures of the lowest energy transition states (bottom). Ade, adenine; and Rib, ribose.

(C) Activation barriers for competing intermolecular hydride transfer or C-alkylation calculated for truncated model structures.

Please cite this article in press as: Mayer and Moran, Metal ions turn on a stereoselective nonenzymatic reduction of keto acids by the coenzyme NADH, Chem (2024), https://doi.org/10.1016/j.chempr.2024.05.007

observation made here is the first example of chirality transfer in a nonenzymatic context between a coenzyme and its biological substrate and furthermore demonstrates the potential for asymmetric induction of the ubiquitous adenosyl cofactor scaffold without requiring complex proteins.[50] Our observation is especially important to the question of how the homochirality observed in biology propagated at the emergence of metabolism and life. The chirality in NADH comes from the ribose in its two nucleoside units. Under prebiotic conditions, nucleosides such as the adenosine fragment found in NADH can be synthesized from ribo-amino-oxazolines,[51] which have recently been shown to be obtainable in homochiral form.[52]

To rationalize the experimentally observed preference for R-lactate formation and the deterioration of stereoselectivity during the reaction, we computationally modeled the key steps of the reduction catalyzed by Al^{3+}. The diphosphate motif of NADH and the keto acid are both suitable ligands for transition metals, and their coordination with aluminum has been studied experimentally.[53,54] Thus, we initially modeled the intramolecular hydride transfer within a pre-arranged complex of these three species (Figure 4B), as the small concentration dependency of the reaction furthermore supports an intramolecular mechanism; we also obtained experimental evidence for such a complex by mass spectrometry (supplemental information, section analysis of key complexes). A key challenge of the computational investigation is the excessive number of stereoisomeric complexes and their conformational flexibility (for details, see section computational study of the supplemental information). However, systematic modeling of large ensembles of conformers for each stereoisomeric transition state allowed us to identify plausible transition structures that show a small preference for forming R-lactate through an intramolecular hydride-transfer pathway (Figure 4B, right; $\Delta\Delta G^{\ddagger}_{calc}$ = 2.7 kJ mol^{-1}; $\Delta\Delta G^{\ddagger}_{exp}$ = 1.7 kJ mol^{-1}). Our computations illustrate that very few stereoisomeric complexes can undergo energetically favored intramolecular hydride transfer (Figure 4B, right). As we observed large amounts of the oxidized pyridinium salts **4**/**I6** (cf. section side product analysis of the Al^{3+}-catalyzed reaction of NADH and pyruvate in the supplemental information), we additionally investigated hydride transfer with the C-adduct **I3** acting as a reductant (see Figure 3C for the structure). In analogous computations for intramolecular hydride transfer starting from **I3** as done with NADH, a slightly higher selectivity for R-lactate formation is suggested ($\Delta\Delta G^{\ddagger}_{calc}$ = 5.3 kJ mol^{-1}). Thus, C-alkylation and the change in reductant cannot alone account for the deterioration of stereoselectivity in an *intra*molecular pathway.

Aside from *intra*molecular hydride transfer within a pre-organized complex, *inter*-molecular hydride transfer is also possible. Due to the system size and the excessive number of potentially reactive species, intermolecular hydride transfer was computationally investigated only on the model structures **M** and **M3** (Figure 4C; see section computational study in the supplemental information and Figures S187 and S188 for the full energy profiles). Notably, the alkylated nicotinamide **M3** is computed to be a more nucleophilic hydride donor than **M** in intermolecular hydride transfer, in line with a previous thermochemical analysis of 5-methylated dihydronicotinamides.[55] This contrasts with the computations for intramolecular hydride transfer in Figure 4B, which suggest a higher barrier with **I3** than with NADH (89.5 vs. 65.5 kJ mol^{-1}). Thus, once formed, **I3** outcompetes NADH as a nucleophile in *inter*molecular hydride transfer but not *intra*molecular hydride transfer. We assume that the intermolecular hydride transfer from **I3** is proceeding

without large stereoselectivity, accounting for the experimentally observed decline in *ee* with increased reaction times.

Conclusions

Catalytic amounts of salts of the two most abundant metals in the Earth's crust (Al^{3+}, $Fe^{2+/3+}$) can partially replace the function of complex enzymes in the nonenzymatic reduction of keto acids by the cofactor NADH in water. The metal ions mimic multiple essential functions of enzymes. They activate the keto acids and pre-organize their interaction with NADH, which accounts for the observed stereoselectivity arising from an intramolecular hydride transfer pathway. Yet, our reaction conditions only provide a starting point for the evolution of metabolism using coenzymes: the observation of side pathways and incomplete transfer of chirality in the nonenzymatic reaction shows the benefits of confining the reactants within ribozymes or enzymes.

There is broad disagreement on whether genetic molecules predated metabolism during the origin of life (i.e., the RNA world hypothesis) or the other way around. However, genetic molecules and metabolic function are both ultimately needed for the emergence of biochemistry. The present stereoselective and nonenzymatic metabolic reaction involving RNA-derived cofactors enabled by metals provides a long-sought missing link between the metabolic and genetic worlds within prebiotic chemistry.

EXPERIMENTAL PROCEDURES

Resource availability

Lead contact

Requests for further information and resources should be directed to and will be fulfilled by the lead contact, Joseph Moran (moran@unistra.fr).

Materials availability

This study did not generate new unique reagents. The products generated by the reported reactions are commercially available.

Data and code availability

All data supporting this study are available in the manuscript or supplemental information.

SUPPLEMENTAL INFORMATION

Supplemental information can be found online at https://doi.org/10.1016/j.chempr.2024.05.007.

ACKNOWLEDGMENTS

This project has received funding from the European Research Council (ERC) under the European Union's Horizon 2020 research and innovation program (grant agreement no 101001752). R.J.M. thanks the Deutsche Forschungsgemeinschaft (DFG, German Research Foundation) for a fellowship (MA 9687/1-1). J.M. thanks the VW Foundation (no. 96_742) for their generous support. Computations were performed at the High-Performance Computing Center of the University of Strasbourg. A part of the computing resources was funded by the Equipex Equip@Meso project (Programme Investissements d'Avenir) and the CPER Alsacalcul/Big Data. The authors thank Dr. Claudia Bonfio, Dr. Quentin Dherbassy, Dr. Claude Legault, Dr. Giulio

Ragazzon, and Maciej Piejko for helpful discussion and proofreading of the manuscript, and Wahnyalo Kazone for help with LC/MS measurements.

AUTHOR CONTRIBUTIONS

R.J.M. and J.M. jointly conceptualized the overall project. R.J.M. conceived the experimental methodology and performed all experiments and computations. The manuscript was written by R.J.M. and J.M.

DECLARATION OF INTERESTS

The authors declare no competing interests.

Received: January 13, 2024
Revised: March 27, 2024
Accepted: May 16, 2024
Published: June 11, 2024

REFERENCES

1. Kirschning, A. (2021). Coenzymes and Their Role in the Evolution of Life. Angew. Chem. Int. Ed. Engl. *60*, 6242–6269. https://doi.org/10.1002/anie.201914786.

2. White, H.B. (1976). Coenzymes as fossils of an earlier metabolic state. J. Mol. Evol. *7*, 101–104. https://doi.org/10.1007/BF01732468.

3. Goldman, A.D., and Kacar, B. (2021). Cofactors are Remnants of Life's Origin and Early Evolution. J. Mol. Evol. *89*, 127–133. https://doi.org/10.1007/s00239-020-09988-4.

4. Benner, S.A., Ellington, A.D., and Tauer, A. (1989). Modern metabolism as a palimpsest of the RNA world. Proc. Natl. Acad. Sci. USA *86*, 7054–7058. https://doi.org/10.1073/pnas.86.18.7054.

5. Fontecilla-Camps, J.C. (2019). Geochemical Continuity and Catalyst/Cofactor Replacement in the Emergence and Evolution of Life. Angew. Chem. Int. Ed. Engl. *58*, 42–48. https://doi.org/10.1002/anie.201808438.

6. McMurry, J., and Begley, T.P. (2016). The Organic Chemistry of Biological Pathways, Second Edition (Roberts and Company Publishers).

7. Metzler, D.E. (2003). Biochemistry: the Chemical Reactions of Living Cells, Second Edition (Academic Press).

8. Houtkooper, R.H., Cantó, C., Wanders, R.J., and Auwerx, J. (2010). The Secret Life of NAD^+: An Old Metabolite Controlling New Metabolic Signaling Pathways. Endocr. Rev. *31*, 194–223. https://doi.org/10.1210/er.2009-0026.

9. Xavier, J.C., Hordijk, W., Kauffman, S., Steel, M., and Martin, W.F. (2020). Autocatalytic chemical networks at the origin of metabolism. Proc. Biol. Sci. *287*, 20192377. https://doi.org/10.1098/rspb.2019.2377.

10. Xavier, J.C., and Kauffman, S. (2022). Small-molecule autocatalytic networks are universal metabolic fossils. Philos. Trans. A Math. Phys. Eng. Sci. *380*, 20210244. https://doi.org/10.1098/rsta.2021.0244.

11. Kirschning, A. (2022). On the evolution of coenzyme biosynthesis. Nat. Prod. Rep. *39*, 2175–2199. https://doi.org/10.1039/D2NP00037G.

12. Rauscher, S.A., and Moran, J. (2022). Hydrogen Drives Part of the Reverse Krebs Cycle under Metal or Meteorite Catalysis. Angew. Chem. Int. Ed. Engl. *61*, e202212932. https://doi.org/10.1002/anie.202212932.

13. Wang, X., Saba, T., Yiu, H.H.P., Howe, R.F., Anderson, J.A., and Shi, J. (2017). Cofactor NAD(P)H Regeneration Inspired by Heterogeneous Pathways. Chem *2*, 621–654. https://doi.org/10.1016/j.chempr.2017.04.009.

14. Dalai, P., and Sahai, N. (2020). A Model Protometabolic Pathway across Protocell Membranes Assisted by Photocatalytic Minerals. J. Phys. Chem. C *124*, 1469–1477. https://doi.org/10.1021/acs.jpcc.9b10127.

15. Basak, S., Nader, S., and Mansy, S.S. (2021). Protometabolic Reduction of NAD^+ with α-Keto Acids. JACS Au *1*, 371–374. https://doi.org/10.1021/jacsau.0c00124.

16. Henriques Pereira, D.P., Leethaus, J., Beyazay, T., do Nascimento Vieira, A., Kleinermanns, K., Tüysüz, H., Martin, W.F., and Preiner, M. (2022). Role of geochemical protoenzymes (geozymes) in primordial metabolism: specific abiotic hydride transfer by metals to the biological redox cofactor NAD^+. FEBS Journal *289*, 3148–3162. https://doi.org/10.1111/febs.16329.

17. Weber, J.M., Henderson, B.L., LaRowe, D.E., Goldman, A.D., Perl, S.M., Billings, K., and Barge, L.M. (2022). Testing Abiotic Reduction of NAD^+ Directly Mediated by Iron/Sulfur Minerals. Astrobiology *22*, 25–34. https://doi.org/10.1089/ast.2021.0035.

18. Summers, D.P., and Rodoni, D. (2015). Vesicle Encapsulation of a Nonbiological Photochemical System Capable of Reducing NAD^+ to NADH. Langmuir *31*, 10633–10637. https://doi.org/10.1021/la502003j.

19. Dowler, M.J., Fuller, W.D., Orgel, L.E., and Sanchez, R.A. (1970). Prebiotic Synthesis of Propiolaldehyde and Nicotinamide. Science *169*, 1320–1321. https://doi.org/10.1126/science.169.3952.1320.

20. Friedmann, N., Miller, S.L., and Sanchez, R.A. (1971). Primitive Earth Synthesis of Nicotinic Acid Derivatives. Science *171*, 1026–1027. https://doi.org/10.1126/science.171.3975.1026.

21. Cleaves, H.J., and Miller, S.L. (2001). The Nicotinamide Biosynthetic Pathway Is a By-Product of the RNA World. J. Mol. Evol. *52*, 73–77. https://doi.org/10.1007/s002390010135.

22. Kim, H.-J., and Benner, S.A. (2018). A Direct Prebiotic Synthesis of Nicotinamide Nucleotide. Chem. Eur. J. *24*, 581–584. https://doi.org/10.1002/chem.201705394.

23. Oba, Y., Takano, Y., Furukawa, Y., Koga, T., Glavin, D.P., Dworkin, J.P., and Naraoka, H. (2022). Identifying the wide diversity of extraterrestrial purine and pyrimidine nucleobases in carbonaceous meteorites. Nat. Commun. *13*, 2008. https://doi.org/10.1038/s41467-022-29612-x.

24. Powner, M.W., Sutherland, J.D., and Szostak, J.W. (2010). Chemoselective Multicomponent One-Pot Assembly of Purine Precursors in Water. J. Am. Chem. Soc. *132*, 16677–16688. https://doi.org/10.1021/ja108197s.

25. Becker, S., Thoma, I., Deutsch, A., Gehrke, T., Mayer, P., Zipse, H., and Carell, T. (2016). A high-yielding, strictly regioselective prebiotic purine nucleoside formation pathway. Science *352*, 833–836. https://doi.org/10.1126/science.aad2808.

26. Becker, S., Feldmann, J., Wiedemann, S., Okamura, H., Schneider, C., Iwan, K., Crisp, A., Rossa, M., Amatov, T., and Carell, T. (2019). Unified prebiotically plausible synthesis of pyrimidine and purine RNA ribonucleotides. Science *366*, 76–82. https://doi.org/10.1126/science.aax2747.

27. Huang, F., Bugg, C.W., and Yarus, M. (2000). RNA-Catalyzed CoA, NAD, and FAD Synthesis from Phosphopantetheine, NMN, and FMN. Biochemistry *39*, 15548–15555. https://doi.org/10.1021/bi002061f.

28. Bonfio, C., Godino, E., Corsini, M., Fabrizi De Biani, F., Guella, G., and Mansy, S.S. (2018). Prebiotic iron–sulfur peptide catalysts generate a pH gradient across model membranes of late protocells. Nat. Catal. *1*, 616–623. https://doi.org/10.1038/s41929-018-0116-3.

29. Hsiao, C., Chou, I.-C., Okafor, C.D., Bowman, J.C., O'Neill, E.B., Athavale, S.S., Petrov, A.S., Hud, N.V., Wartell, R.M., Harvey, S.C., and Williams, L.D. (2013). RNA with iron(II) as a cofactor catalyses electron transfer. Nat. Chem. *5*, 525–528. https://doi.org/10.1038/nchem.1649.

30. Tsukiji, S., Pattnaik, S.B., and Suga, H. (2004). Reduction of an Aldehyde by a NADH/Zn^{2+}-Dependent Redox Active Ribozyme. J. Am. Chem. Soc. *126*, 5044–5045. https://doi.org/10.1021/ja0495213.

31. Chipman, D.M., Yaniv, R., and Van Eikeren, P. (1980). Models for nicotinamide coenzymes. Isotope effect discrepancies in the reaction of dihydronicotinamides with trifluoroacetophenone are due to adduct formation. J. Am. Chem. Soc. *102*, 3244–3246. https://doi.org/10.1021/ja00529a060.

32. Nogal, N., Luis-Barrera, J., Vela-Gallego, S., Aguilar-Galindo, F., and De La Escosura, A.; During the revisions of this paper, the nonenzymatic reductive amination of keto acids with NADH as the hydride donor was reported, which relies on the higher electrophilicity of iminium ions compared to carbonyl compounds: (2024). NADH-mediated primordial synthesis of amino acids. Org. Chem. Front. *11*, 1924–1932. https://doi.org/10.1039/D4QO00050A.

33. Mauzerall, D., and Westheimer, F.H. (1955). 1-Benzyldihydronicotinamide—A Model for Reduced DPN. J. Am. Chem. Soc. *77*, 2261–2264. https://doi.org/10.1021/ja01613a070.

34. Mayer, R.J., and Moran, J. (2022). Quantifying Reductive Amination in Nonenzymatic Amino Acid Synthesis. Angew. Chem. Int. Ed. *61*, e202212237. https://doi.org/10.1002/anie.202212237.

35. Oppenheimer, N.J., and Kaplan, N.O. (1974). Structure of the primary acid rearrangement product of reduced nicotinamide adenine dinucleotide (NADH). Biochemistry *13*, 4675–4685. https://doi.org/10.1021/bi00720a001.

36. Plapp, B.V., Savarimuthu, B.R., Ferraro, D.J., Rubach, J.K., Brown, E.N., and Ramaswamy, S. (2017). Horse Liver Alcohol Dehydrogenase: Zinc Coordination and Catalysis. Biochemistry *56*, 3632–3646. https://doi.org/10.1021/acs.biochem.7b00446.

37. Yasui, S., and Ohno, A. (1986). Model studies with nicotinamide derivatives. Bioorg. Chem. *14*, 70–96. https://doi.org/10.1016/0045-2068(86)90019-2.

38. Ohno, A., and Ushida, S. (1986). Mechanistic Models of Asymmetric Reductions (Springer). https://doi.org/10.1007/978-3-642-48868-9.

39. Inouye, Y., Oda, J., and Baba, N. (1983). Reductions with Chiral Dihydropyridine Reagents. In Asymmetric Synthesis (Elsevier), pp. 91–124. https://doi.org/10.1016/B978-0-12-507702-6.50009-8.

40. Paul, C.E., Arends, I.W.C.E., and Hollmann, F. (2014). Is Simpler Better? Synthetic Nicotinamide Cofactor Analogues for Redox Chemistry. ACS Catal. *4*, 788–797. https://doi.org/10.1021/cs4011056.

41. McSkimming, A., and Colbran, S.B. (2013). The coordination chemistry of organo-hydride donors: new prospects for efficient multi-electron reduction. Chem. Soc. Rev. *42*, 5439–5488. https://doi.org/10.1039/c3cs35466k.

42. Calvin, M. (1959). Evolution of Enzymes and the Photosynthetic Apparatus: Primitive photochemistry and porphyrin catalysis after separate genesis join in modern photosynthesis. Science *130*, 1170–1174. https://doi.org/10.1126/science.130.3383.1170.

43. De Graaf, R., De Decker, Y., Sojo, V., and Hudson, R. (2023). Quantifying Catalysis at the Origin of Life. Chem. Eur. J. *29*, e202301447. https://doi.org/10.1002/chem.202301447.

44. Beyazay, T., Belthle, K.S., Farès, C., Preiner, M., Moran, J., Martin, W.F., and Tüysüz, H. (2023). Ambient temperature CO_2 fixation to pyruvate and subsequently to citramalate over iron and nickel nanoparticles. Nat. Commun. *14*, 570. https://doi.org/10.1038/s41467-023-36088-w.

45. Forsythe, J.G., Petrov, A.S., Millar, W.C., Yu, S.-S., Krishnamurthy, R., Grover, M.A., Hud, N.V., and Fernández, F.M. (2017). Surveying the sequence diversity of model prebiotic peptides by mass spectrometry. Proc. Natl. Acad. Sci. USA *114*, E7652–E7659. https://doi.org/10.1073/pnas.1711631114.

46. Nordstrom, D.K., and May, H.M. (1995). Complex stability constants summarized by Nordstrom et al. suggest that keto acids are by 9 to 15 orders of magnitude stronger ligands compared to acetate. Accordingly, with the employed concentrations of pyruvate (**1a**) and acetate, Al^{3+} is expected to be almost exclusively coordinated by **1a**. Yet, with stronger coordinating buffers, differences due to the reduced availability of aluminum are to be expected. Aqueous Equilibrium Data for Mononuclear Aluminum Species. In The Environmental Chemistry of Aluminum, G. Sposito, ed. (CRC Press), pp. 39–80. https://doi.org/10.1201/9780138736781-2.

47. Burés, J. (2016). Variable Time Normalization Analysis: General Graphical Elucidation of Reaction Orders from Concentration Profiles. Angew. Chem. Int. Ed. *55*, 16084–16087. https://doi.org/10.1002/anie.201609757.

48. Aizpurua, J.M., Palomo, C., Fratila, R.M., Ferrón, P., Benito, A., Gómez-Bengoa, E., Miranda, J.I., and Santos, J.I. (2009). Mechanistic Insights on the Magnesium(II) Ion-Activated Reduction of Methyl Benzoylformate with Chelated NADH Peptide β-Lactam Models. J. Org. Chem. *74*, 6691–6702. https://doi.org/10.1021/jo901236d.

49. Ding, X., Lin, S., Weng, H., and Liang, J. (2018). Separation and determination of the enantiomers of lactic acid and 2-hydroxyglutaric acid by chiral derivatization combined with gas chromatography and mass spectrometry. J. Sep. Sci. *41*, 2576–2584. https://doi.org/10.1002/jssc.201701555.

50. Wang, C., Qi, Q., Li, W., Dang, J., Hao, M., Lv, S., Dong, X., Gu, Y., Wu, P., Zhang, W., et al. (2020). A Cu(II)–ATP complex efficiently catalyses enantioselective Diels–Alder reactions. Nat. Commun. *11*, 4792. https://doi.org/10.1038/s41467-020-18554-x.

51. Xu, J., Green, N.J., Russell, D.A., Liu, Z., and Sutherland, J.D. (2021). Prebiotic Photochemical Coproduction of Purine Ribo- and Deoxyribonucleosides. J. Am. Chem. Soc. *143*, 14482–14486. https://doi.org/10.1021/jacs.1c07403.

52. Ozturk, S.F., Liu, Z., Sutherland, J.D., and Sasselov, D.D. (2023). Origin of biological homochirality by crystallization of an RNA precursor on a magnetic surface. Sci. Adv. *9*, eadg8274. https://doi.org/10.1126/sciadv.adg8274.

53. Yang, X., Zhang, Q., Li, L., and Shen, R. (2007). Structural features of aluminium(III) complexes with bioligands in glutamate dehydrogenase reaction system – a review. J. Inorg. Biochem. *101*, 1242–1250. https://doi.org/10.1016/j.jinorgbio.2007.06.030.

54. Forsberg, O., Gelland, B., Ulmgren, P., and Wahlberg, O. (1978). Equilibrium Studies of the Pyruvate Protonation and Metal Pyruvate Complexes in Aqueous Solutions. Acta Chem. Scand. *32a*, 345–352. https://doi.org/10.3891/acta.chem.scand.32a-0345.

55. Zhu, X.-Q., Tan, Y., and Cao, C.-T. (2010). Thermodynamic Diagnosis of the Properties and Mechanism of Dihydropyridine-Type Compounds as Hydride Source in Acetonitrile with "Molecule ID Card.". J. Phys. Chem. B *114*, 2058–2075. https://doi.org/10.1021/jp911137p.